JACS ARTICLES
Published on Web 12/09/2005

Vacuum Ultraviolet Photoionization of C_3

Christophe Nicolas,[†] Jinian Shu,[†] Darcy S. Peterka,[†,‡] Majdi Hochlaf,[§] Lionel Poisson,[†,||] Stephen R. Leone,[†,‡] and Musahid Ahmed*,[†]

Contribution from the Chemical Sciences Division, Ernest Orlando Lawrence Berkeley National Laboratory, Berkeley, California 94720, Department of Chemistry and Physics, University of California, Berkeley, California 94720, and Laboratoire de Chimie Théorique, Université de Marne la Vallée, F 77454 - Champs sur Marne, France

Received August 19, 2005; E-mail: mahmed@lbl.gov

Abstract: Photoionization efficiency (PIE) curves for C_3 molecules produced by laser ablation are measured from 11.0 to 13.5 eV with tunable vacuum ultraviolet undulator radiation. A step in the PIE curve versus photon energy, obtained with N_2 as the carrier gas, supports the conclusion of very effective cooling of C_3 to its linear $^1\Sigma_g^+$ ground state. The second step observed in the PIE curve versus photon energy could be the first experimental evidence of the $C_3^+(^2\Sigma_g^+)$ excited state. The experimental results, complemented by ab initio calculations, suggest a state-to-state vertical ionization energy of 11.70 $\pm$ 0.05 eV between the $C_3(\tilde{X}^1\Sigma_g^+)$ and the $C_3^+(\tilde{X}^2\Sigma_u^+)$ states. An ionization energy of 11.61 $\pm$ 0.07 eV between the neutral and ionic ground states of C_3 is deduced using the data together with our calculations. Accurate ab initio calculations are performed for both linear and bent geometries on the lowest doublet electronic states of C_3^+ using Configuration Interaction (CI) approaches and large basis sets. These calculations confirm that C_3^+ is bent in its electronic ground state, which is separated by a small potential barrier from the $^2\Sigma_u^+$ minimum. The gradual increase at the onset of the PIE curve suggests a geometry change between the ground neutral and cationic states. The energies between several doublet states of the ion are theoretically determined to be 0.81, 1.49, and 1.98 eV between the $^2\Sigma_u^+$ and the $^2\Sigma_g^+$, $^2\Pi_u$, $^2\Pi_g$ excited states of C_3^+, respectively.

Introduction

Small carbon clusters play an important role in our environment, as precursors of soot and large carbon-containing molecules, including aromatic species and fullerenes, and also in astrochemistry. The C_3 molecule is thought to be an ubiquitous precursor in a variety of astrophysical systems.[1] The first spectroscopic observation of C_3 emission, due to the $\tilde{A}^1\Pi_u$-$\tilde{X}^1\Sigma_g^+$ band, was reported over a century ago when Huggins investigated the spectra of a comet tail. The same spectrum is also seen in absorption in cool carbon stars and via the ν_3 vibration−rotation band in circumstellar shells.[2]

Considerable theoretical and experimental work is dedicated to the $C_3(\tilde{X}^1\Sigma_g^+)$ ground state and the ($\tilde{A}^1\Pi_u$, $\tilde{a}^3\Pi_u$, $\tilde{b}^3\Pi_g$, $^1\Sigma^+_u$) electronically excited states of C_3.[3−5] Spectroscopic studies of C_3 show that its electronic ground state presents a linear equilibrium geometry. Recent ab initio calculations find the equilibrium C−C bond lengths to be in the range 1.296−1.301 Å,[5,6] in good agreement with the measured value 1.297 Å.[2] The $\tilde{A}^1\Pi_u$-$\tilde{X}^1\Sigma_g^+$ system has been studied extensively.[2−4,7−9] The first electronically excited state, $\tilde{A}^1\Pi_u$, lying ~3 eV above the ground state, possesses a linear equilibrium geometry and exhibits a large Renner−Teller effect.[10] The $^1\Sigma_u^+$−$\tilde{X}^1\Sigma_g^+$ system was observed in the early 1980's by Chang and Graham[11] and was confirmed by a recent matrix-isolation study.[12] These studies highlighted the existence of strong couplings between the $^1\Sigma_u^+$ and the $\tilde{A}^1\Pi_u$ states and also with the nearest triplet states. Two metastable triplet states, $\tilde{a}^3\Pi_u$ and $\tilde{b}^3\Pi_g$, have been detected in matrix and gas-phase studies.[12,13] The $\tilde{b}^3\Pi_g$ state is less well-known, even though gas-phase vibronic transitions of the $\tilde{b}^3\Pi_g$-$\tilde{a}^3\Pi_u$ system have been observed.[14,15] Recent theoretical studies investigated the lower singlet potential-energy surfaces[5,6] and

† Ernest Orlando Lawrence Berkeley National Laboratory.
‡ University of California.
§ Université de Marne la Vallée.
|| Permanent address: Laboratoire Francis Perrin, CEA/DSM/DRECAM/SPAM − CNRS URA 2453, 91191 Gif-sur-Yvette, France.

(1) Savic, I.; Cermak, I.; Gerlich, D. *Int. J. Mass. Spectrom.* **2005**, *240*, 139−147.
(2) Hinkle, K. W.; Keady, J. J.; Bernath, P. F. *Science* **1988**, *241*, 1319−1322.
(3) Weltner, W.; Vanzee, R. J. *Chem. Rev.* **1989**, *89*, 1713−1747.
(4) Van Orden, A.; Saykally, R. J. *Chem. Rev.* **1998**, *98*, 2313−2357.
(5) Fueno, H.; Taniguchi, Y. *Chem. Phys. Lett.* **1999**, *312*, 65−70.
(6) Ahmed, K.; Balint-Kurti, G. G.; Western, C. M. *J. Chem. Phys.* **2004**, *121*, 10041−10051.
(7) Hoshina, H.; Kato, Y.; Morisawa, Y.; Wakabayashi, T.; Momose, T. *Chem. Phys.* **2004**, *300*, 69−77.
(8) Tanabashi, A.; Hirao, T.; Amano, T.; Bernath, P. F. *Astrophys. J.* **2005**, *624*, 1116−1120.
(9) Zhang, G. Q.; Chen, K. S.; Merer, A. J.; Hsu, Y. C.; Chen, W. J.; Shaji, S.; Liao, Y. A. *J. Chem. Phys.* **2005**, 122.
(10) Jungen, C.; Merer, A. J. *Mol. Phys.* **1980**, *40*, 95−114.
(11) Chang, K. W.; Graham, W. R. M. *J. Chem. Phys.* **1982**, *77*, 4300−4303.
(12) Monninger, G.; Forderer, M.; Gurtler, P.; Kalhofer, S.; Petersen, S.; Nemes, L.; Szalay, P. G.; Kratschmer, W. *J. Phys. Chem. A* **2002**, *106*, 5779−5788.
(13) Cermak, I.; Forderer, M.; Cermakova, I.; Kalhofer, S.; Stopka-Ebeler, H.; Monninger, G.; Kratschmer, W. *J. Chem. Phys.* **1998**, *108*, 10129−10142.
(14) Sasada, H.; Amano, T.; Jarman, C.; Bernath, P. F. *J. Chem. Phys.* **1991**, *94*, 2401−2407.
(15) Tokaryk, D. W.; Civis, S. *J. Chem. Phys.* **1995**, *103*, 3928−3941.

10.1021/ja055430+ CCC: $33.50

the triplet excited states of C_3.[5,16] As has been shown in experimental matrix-isolated C_3 studies,[12,13,17] these two manifolds interact together, strongly complicating the theoretical interpretation of the data.

Two review articles on carbon clusters[3,4] reveal the paucity of data when it comes to the C_3^+ molecule. In the late 1980's, doubt existed about the geometry of the ground state, due to different interpretations of the experimental results derived from a Coulombic explosion imaging study.[18,19] Recent calculations agree that the ground state is bent, with a $^2B_2$ C_{2v} structure, and the equilibrium angle is found to be between 66° and 68.2°, depending on the calculation method.[20,21] The energy of the next higher $^2\Sigma_u^+$ $D_{\infty h}$ linear isomer strongly depends on the calculation method: 0.09 eV[20] from the BP86/6-31(d) and 0.4 eV[21] from the CCSD(T) aug-cc-pVTZ methods. Generally, theoretical treatments of the C_n^+ molecule are difficult, due to spatial symmetry breaking problems.[20] In this paper we present a new set of high level ab initio calculations on C_3^+, which consists of one-dimensional cuts of the potential energy surfaces of its lowest doublet states along the stretching and the bending coordinates. These calculations are performed at the Complete Active Space Self-Consistent Field (CASSCF) and Multi-Reference Configuration Interaction (MRCI) level.

Despite the impressive amount of theoretical and experimental work performed on neutral and cationic C_3, simple physical properties, such as its ionization energy (IE), are not very well-known. There are a few experimental values for the IE in the literature. Ramanathan et al.[22] report an adiabatic value of 13.0 $\pm$ 0.1 eV using charge-transfer methods. Rohlfing et al.,[23] using laser multiphoton ionization of neutral clusters in a molecular beam, provide a "coarse" bracketing of the IE value between 9.98 and 11.61 eV. Some early work, in sublimation cells, also gave appearance energy values of 11.5 $\pm$ 0.1 eV,[24] 12.1 $\pm$ 0.3 eV,[25] and 12.6 $\pm$ 0.6 eV.[26]

There have been no direct photoionization efficiency curves (PIE) recorded or photoionization energies measured for the C_3 molecule. In this work, the C_3 IE has been determined by recording PIE curves with tunable vacuum ultraviolet (VUV) undulator radiation at the Advanced Light Source, between 11.0 and 13.5 eV. Neutral C_3 molecules can be excited to various electronically excited states when created by laser ablation. Different types of buffer gases, such as He, Ar, N_2, or CO_2, are used to find the optimal quenching of these states. Jet-cooled experiments coupled with high level ab initio calculations, as described here, will help to unravel the intricacies of the structures observed in the PIE curve of C_3. This will provide a glimpse into the complicated nature of the C_3 electronic states involved in the photoionization process.

Experimental Setup

The experiments are performed on a laser ablation apparatus coupled to a 3 m monochromator on the Chemical Dynamics Beamline[27] at the Advanced Light Source. The apparatus is based on a modified design of a crossed molecular beams machine and consists of a six-way cross with 33.66 cm conflat dimensions.[28] Four 6.99 cm conflat ports in the same plane provide access for lasers and synchrotron radiation. A source chamber couples to the main chamber, via a 33.66 cm conflat, and all components key in to provide alignment for the molecular beam with respect to the synchrotron beam. The source region has two ports for access of lasers to the front of the pulsed valve for ablation studies. A motor mount based on the design of Kaiser and Suits[29] allows for ablation rods to be rotated and translated simultaneously just in front of the nozzle. This configuration has been used successfully to measure ionization energies of laser ablated refractory metal oxides recently.[30] Two magnetically levitated turbo molecular pumps (Seiko Seiki) with 2000 L/s and 1000 L/s pumping speeds are connected to the source and main chamber, respectively. During operation of the ablation experiment with He as the carrier gas, the pressures in the source, main, and synchrotron regions are 2.0×10^{-5}, 2×10^{-7}, and 1×10^{-8} Torr, respectively (1 Torr = 133.32 Pa).

Carbon species such as C, C_2, and C_3 are generated by ablation of a free-running, rotating, and translating graphite rod (99.995%, 6 mm diameter from Aldrich). The ablated species are entrained in a supersonic expansion using He, N_2, Ar, or CO_2 as carrier gases, originating from a piezo-electric pulsed valve operating at 100 Hz and synchronized with the arrival of 532 nm photons generated by the second harmonic of a Nd:YAG laser (Coherent Infinity). The laser power was 5 mJ per pulse in 3 ns, focused down to a spot of ~1.5 mm diameter using a 1 m lens. The experimental conditions, such as laser power and delay between the pulsed valve and the ablation laser, are chosen to obtain carbon species only up to C_3, thus avoiding contamination of the C_3 PIE by dissociative photoionization of larger clusters.

A pair of deflection plates located between the rod and skimmer assembly remove all charged species generated by the ablation process, allowing only a neutral beam to pass through the differential pumping wall (1 mm skimmer hole) separating the source chamber from the main photoionization chamber. Typically 5 counts measured over 180 s come from the ablation laser, corresponding to the effective dark count level of our detector.

The neutral C_3 beam is interrogated in the ionization region of a commercial reflectron mass spectrometer (R. M. Jordan) by the tunable undulator VUV radiation. The photoionization region is situated 9 cm from the nozzle. As the synchrotron light is quasi-continuous (500 MHz), a start pulse for the TOF ion packet is provided by pulsing the ion optics. In general the ion optics are biased in such a fashion that all ions are accelerated away from the detector. Ion signals from the microchannel plate detector are collected with a multichannel-scalar card (FAST Comtec 7886) triggered by the ablation laser pulse. Time-of-flight spectra are recorded for the photoionization energy range between 10.0 and 13.5 eV. The typical step size used for these experiments is 50 meV, and the dwell time is 80 s. We estimate approximately 10^8 molecules s^{-1} are present in the 1 mm^3 ionization region after taking into account the ablation conditions, skimmer geometry, the distance from the ablation and ionization regions, and the length of the buffer gas pulse. The count rates observed by irradiation with 10^{13} photons s^{-1} and assuming unity in collection

(16) Terentyev, A.; Scholz, R.; Schreiber, M.; Seifert, G. *J. Chem. Phys.* **2004**, *121*, 5767−5776.
(17) Zhang, G. Q.; Lin, B. G.; Wen, S. M.; Hsu, Y. C. *J. Chem. Phys.* **2004**, *120*, 3189−3200.
(18) Faibis, A.; Kanter, E. P.; Tack, L. M.; Bakke, E.; Zabransky, B. J. *J. Phys. Chem.* **1987**, *91*, 6445−6447.
(19) Vager, Z.; Kanter, E. P. *J. Phys. Chem.* **1989**, *93*, 7745−7746.
(20) Orlova, G.; Goddard, J. D. *Chem. Phys. Lett.* **2002**, *363*, 486−491.
(21) Fura, A.; Turecek, F.; McLafferty, F. W. *Int. J. Mass. Spectrom.* **2002**, *217*, 81−96.
(22) Ramanathan, R.; Zimmerman, J. A.; Eyler, J. R. *J. Chem. Phys.* **1993**, *98*, 7838−7845.
(23) Rohlfing, E. A.; Cox, D. M.; Kaldor, A. *J. Chem. Phys.* **1984**, *81*, 3322−3330.
(24) Gupta, S. K.; Gingerich, K. A. *J. Chem. Phys.* **1979**, *71*, 3072−3080.
(25) Kohl, F. J.; Stearns, C. A. *J. Chem. Phys.* **1970**, *52*, 6310-&.
(26) Drowart, J.; Burns, R. P.; Demaria, G.; Inghram, M. G. *J. Chem. Phys.* **1959**, *31*, 1131−1132.
(27) Heimann, P. A.; Koike, M.; Hsu, C. W.; Blank, D.; Yang, X. M.; Suits, A. G.; Lee, Y. T.; Evans, M.; Ng, C. Y.; Flaim, C.; Padmore, H. A. *Rev. Sci. Instrum.* **1997**, *68*, 1945−1951.
(28) Ahmed, M.; Blunt, D.; Chen, D.; Suits, A. G. *J. Chem. Phys.* **1997**, *106*, 7617−7624.
(29) Kaiser, R. I.; Suits, A. G. *Rev. Sci. Instrum.* **1995**, *66*, 5405−5411.
(30) Metz, R. B.; Nicolas, C.; Ahmed, M.; Leone, S. R. *J. Chem. Phys.* **2005**, *123*, 114313−114316.

efficiency for the ions suggest that this estimate, while necessarily crude (since the absolute photoionization cross section of C_3 is unknown), is valid.

The PIE curve of C_3 is obtained by adding all the C_3^+ counts in the mass peak at each photon energy, normalized by the photon flux and the number of laser shots. The synchrotron VUV photon flux is measured by a Si photodiode (IRD, SXUV-100).

The PIE curves presented below are obtained by averaging several measurement sets (4−6 scans typically). It is worth noting that due to small variations in the ablation source during the TOF spectra recording time, a dispersion of the measured intensities is observed. While shot-to-shot fluctuations in the laser power would contribute to variations in intensity, it is the physical wobble and surface morphology of the rod that generate the largest scatter in the data set. This is shown quantitatively by the error bars in the following PIE curves, which can reach up to ±20% per 8200 laser shots. Ablation was also attempted with 193 nm excimer laser and 527 nm Nd:YLF laser radiation. However, the best signal-to-noise ratio and stability was observed with 532 nm Nd:YAG laser radiation, and hence these are the reported results.

To calibrate the photon energy, autoionization peaks of Xe and a resonance feature in the PIE curve of C atom are used. This resonance, due to the atomic transition 2p $^3P_{0,1,2}$−2p′ $^3S_1$ at 13.116 eV,[31] has a width close to 6 meV. Therefore the 25 meV fwhm, on average, observed during this study corresponds to the energy resolution.

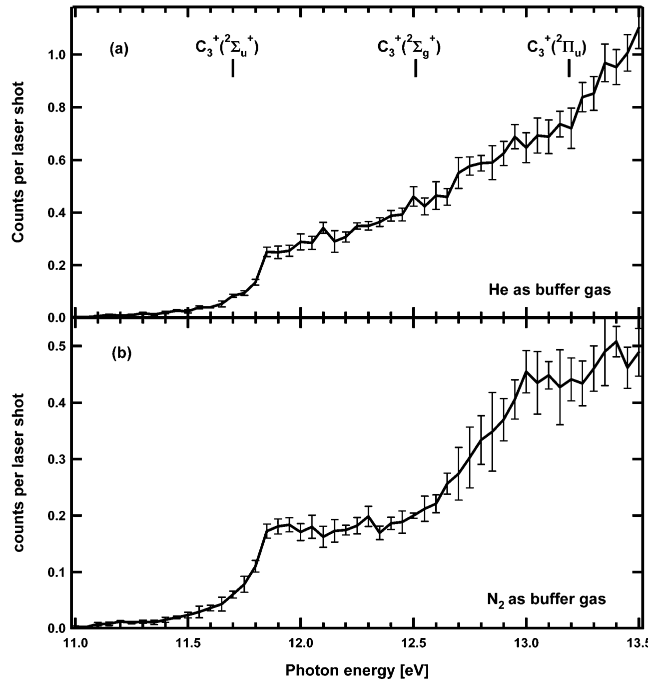

Figure 1. (a) Photoionization efficiency curve of C_3 with He as the buffer gas. The line corresponds to the average of four energy scans. (b) Photoionization efficiency curve of C_3 with N_2 as the buffer gas. The line corresponds to the average of six energy scans. See text for error bar calculation. The CASSCF computed energy positions for the electronically excited states of C_3^+ are marked on top of the figure with vertical bars.

Theoretical Methods

Theoretical treatments of the C_n^+ molecule are difficult because of symmetry breaking problems.[20] Here the one-dimensional cuts on the three-dimensional potential energy surfaces (PESs) of the lowest doublet states of C_3^+ are obtained using the complete active space self-consistent field (CASSCF) and the Multi-Reference Configuration Interaction (MRCI) approaches.[32−34] The higher spin multiplicities are not considered here since they cannot be accessed during single photon ionization from $C_3(\tilde{X}^1\Sigma_g^+)$. In these calculations, the *spdf* subset of the cc-pVQZ basis set of Dunning[35] contracted to [5s, 4p, 3d, 2f] for C, resulting in 138 contracted Gaussian-type orbitals, is used. All valence molecular orbitals are taken into account in the active space. A state-averaged procedure was applied in these CASSCF computations, in which the electronic states have equal weights in the optimization procedure. For MRCI calculations, all configurations having a weight ≥ 0.005 in the CI expansion of the CASSCF wave functions were taken into account as a reference. The electronic structure computations are done with the MOLPRO program suite.[36] In this work, the C_2 axis is chosen to be the *y*-axis for the symmetry designation of the electronic states, and the *x*-axis is out-of-plane.

Results

Photoionization Efficiency (PIE) Spectra. Figure 1 depicts the PIE spectra of C_3 in the 11.0−13.5 eV photon energy range, using He (backing pressure of 15 psi (1 psi = 6.894 kPa)) and N_2 (backing pressures of 50 and 100 psi) as buffer gases. In the case of N_2, the variation of the backing pressure had no influence on the PIE spectra. Different buffer gases are used here in order to achieve an efficient internal cooling of the neutral C_3 molecule. Ar and CO_2 have also been used as carrier gases, with backing pressures of 100 and 18 psi, respectively. The resulting PIE spectra (not shown here) present similar shapes over the whole spectral range as those obtained with He, albeit with lower ion signal levels. The error bars in Figures 1 and 2 are calculated by dividing the maximum intensity difference measured at a fixed photon energy with the square root of the number of measurements.

The PIE spectra present steplike structures. Between the photon energies 11.0 and 11.25 eV, the ion signal is flat and low. Then, with increasing energy, the PIEs show a gradual onset. Detail of the onset is provided in Figure 2, when N_2 is used as the buffer gas. A clear step in the intensity also appears around 11.7 eV, and then the PIE curve reaches a small plateau. At 12.2 eV the curve increases again gradually until 13.2 eV, where a break in the slope is clearly seen. In the 13.2−13.5 eV energy range the increase is much steeper. A determination of the true ionization onset is not trivial, due to the long tail extending from 11.0 to 11.7 eV which could arise from incomplete quenching of electronically and vibrationally excited states of the neutral C_3. The first step onset is, however, easier to determine by the intersection of the photon energy axis with a linear fit. A point fitting procedure is used to generate the error of the onset value as shown in Figure 2. With this method, an onset of 11.70 ± 0.05 eV is derived. The relatively large error lines are due to the fitting procedure and do not correspond to the nominal photon resolution, which is ∼25 meV.

Figure 1a and 1b show that the PIE spectra of C_3 obtained using either He or N_2 possess very similar shapes at low photon energies until the first plateau. But in N_2 the plateau is longer. After 12.4 eV the intensity of C_3^+ ions increases again gradually to reach a second plateau at 12.9 eV. Due to the dispersion in the data, it is difficult to affirm the presence of additional structure between 13.0 and 13.5 eV.

(31) Johansson, L *Ark. Fys.* **1966**, *31*, 201−235.
(32) Knowles, P. J.; Werner, H. J. *Chem. Phys. Lett.* **1985**, *115*, 259−267.
(33) Werner, H. J.; Knowles, P. J. *J. Chem. Phys.* **1988**, *89*, 5803−5814.
(34) Knowles, P. J.; Werner, H. J. *Chem. Phys. Lett.* **1988**, *145*, 514−522.
(35) Dunning, T. H. *J. Chem. Phys.* **1989**, *90*, 1007−1023.
(36) Werner, H.-J. et al. MOLPRO, a package of ab initio programs; Universität Stüttgart and University of Birmingham: Stüttgart, Germany and Birmingham, U.K., 2002. http://www.molpro.net

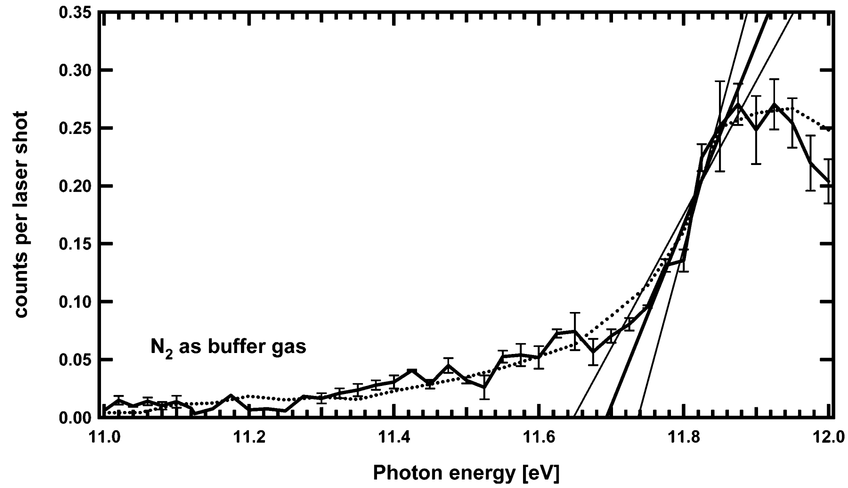

Figure 2. Photoionization efficiency curve of C_3 with N_2 as the buffer gas. The solid line (with the error bars) corresponds to the average of different sets (only one set between 11.10 and 11.24 eV) of measurements with an energy step of 25 meV. For the calculation of the error bars, see text. The dashed line corresponds to the PIE curve depicted in Figure 1b, recorded with an energy step of 50 meV. The thick straight line depicts results from a point fitting procedure used to derive the ionization energy. The thin straight lines on either side constrain the fit and show the relative error.

Table 1. CASSCF Vertical Excitation Energies (T_v) of the Lowest Doublet States of C_3^+

electronic state	T_v (eV)
$^2\Sigma_u^+$	0^a
$^2\Sigma_g^+$	0.81
$^2\Pi_u$	1.49
$^2\Pi_g$	1.98

[a] Total CASSCF energy at the equilibrium geometry of C_3^+ $^2\Sigma_u^+$: −113.200 335 5 au.

More attention is paid to confirm the nature of the shape of the first onset. To check that it is not affected by the scan increment, two scans with smaller step energy sizes (25 meV) were recorded. The resulting averaged PIE curve (solid line) in the 11−12 eV energy range is shown in Figure 2 together with the PIE spectrum of Figure 1b (dashed line). In the 11.10−11.24 eV range only one scan was recorded due to the structureless nature of the PIE at these energies. The error bars are also omitted for this energy range. Figure 2 shows that the dashed and the solid lines coincide within the error bars and that the decrease in the step energy does not influence the onset.

Theoretical Results

The dominant electronic configuration of the ground state ($\tilde{X}^1\Sigma_g^+$) of the neutral C_3 is $(1\sigma_g)^2(1\sigma_u)^2(2\sigma_g)^2(3\sigma_g)^2(2\sigma_u)^2(1\pi_u)^4(4\sigma_g)^2(3\sigma_u)^2$. The removal of one electron from each of the valence orbitals, for instance $3\sigma_u$, $4\sigma_g$, and $1\pi_u$, results in the formation of the $^2\Sigma_u^+$, $^2\Sigma_g^+$, and $^2\Pi_u$ states, respectively. The formation of the lowest $^2\Pi_g$ state corresponds to the removal of an electron from the $3\sigma_u$ along with simultaneous excitation of another electron from the $3\sigma_u$ valence orbital to the $1\pi_g$ vacant orbital.

Table 1 lists the CASSCF vertical excitation energies of the electronically excited states of C_3^+ computed for $R_{CC} = 2.6$ Bohr which is close to the equilibrium R_{CC} distance in C_3^+-($^2A_1$). These energies are given with respect to the C_3^+ ($\tilde{X}^2\Sigma_u^+$) minimum. These values are obtained from state-averaged calculations and should be accurate to within ±0.1 eV.

Figure 3 depicts the collinear CASSCF one-dimensional cuts of the 3-D PESs of the lowest doublet electronic states of C_3^+ along the CC stretch when the other CC stretch is kept fixed at

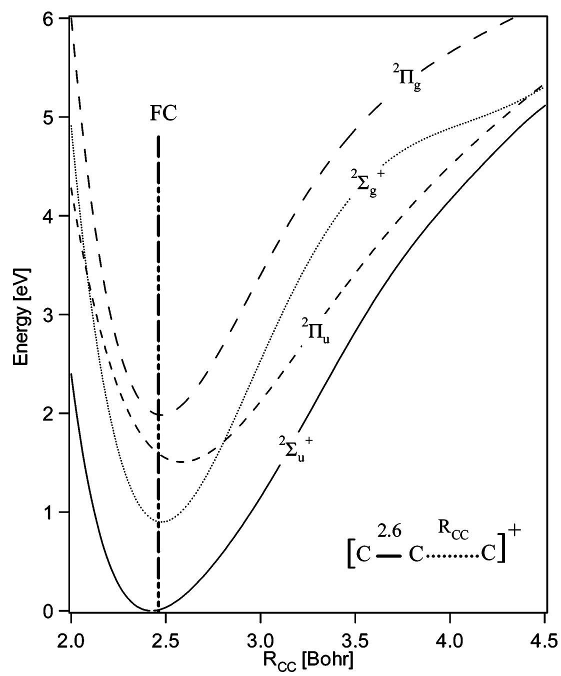

Figure 3. CASSCF potential energy curves of the doublet states of C_3^+ along the CC distance. The other CC distance is fixed at 2.6 Bohr. The g−u symmetry applies only at the CC distance of 2.6 Bohr.

2.6 Bohr. This figure gives an overview of the behavior of the doublet states when one CC distance is stretched. One can see that the doublet states exhibit several avoided crossings and conical intersections. For example, the $^2\Pi_u$ state forms a conical intersection with the $^2\Sigma_g^+$ state at R_{CC} ∼2.8 Bohr; hence in C_s symmetry, the two $^2A'$ components will form an avoided crossing and both states will be coupled by the bending and the antisymmetric stretching modes. The crossing between the $^2\Sigma_g^+$ and $^2\Pi_u$ states is close to the equilibrium geometry of the $^2\Pi_u$ state, complicating the mapping of its 3D-PES. The vertical line corresponds to the middle of the Franck−Condon region defined by the $C_3(\tilde{X}^1\Sigma_g^+)$ (0,0,0) ground-state wave function. At the CASSCF level of theory, the collinear equilibrium bond distances of the electronic states of C_3^+ are computed to be

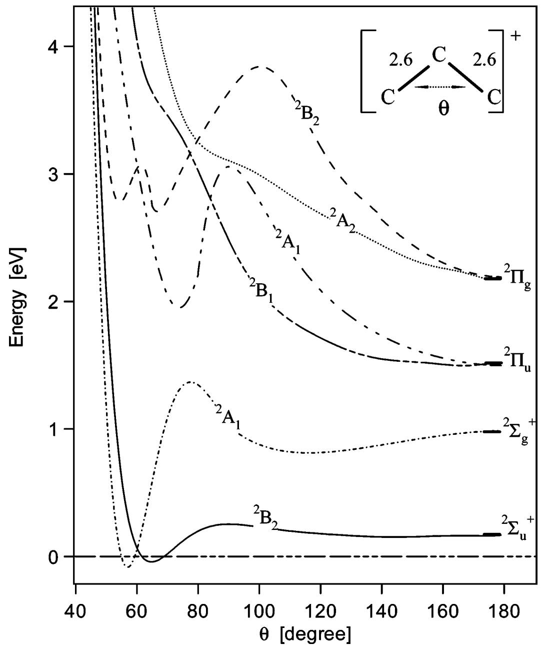

Figure 4. CASSCF potential energy curves of the doublet states of C_3^+ along the bending angle. The zero line corresponds to the CASSCF energy of the $\tilde{X}^2\Sigma_u^+$ for both R_{CC} bond lengths equal to 2.45 Bohr.

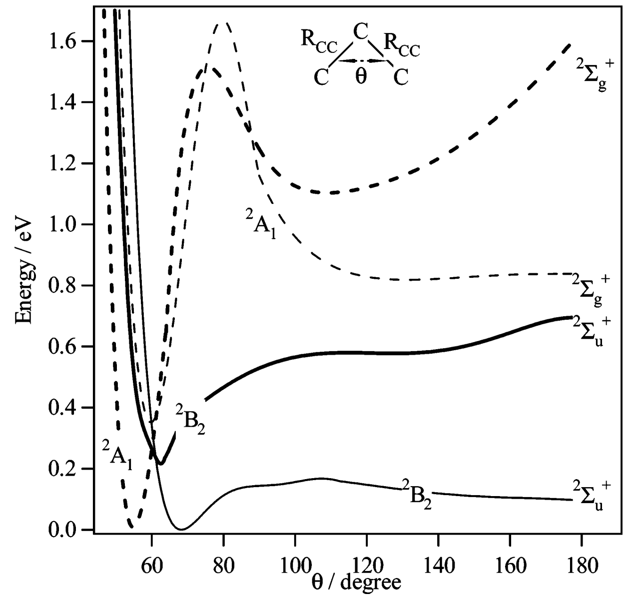

Figure 5. MRCI potential energy curves of the two doublet states of C_3^+ along the bending coordinate. Thick lines: both R_{CC} distances were set to 2.65 Bohr (i.e., approximately their equilibrium values in $^2A_1$). Thin lines: both R_{CC} distances were set to 2.45 Bohr (i.e., approximately their equilibrium values in $^2\Sigma_u^+$, $^2B_2$, and $^2\Sigma_g^+$).

2.42, 2.48, 2.59, and 2.48 (all values are in Bohr) for the $^2\Sigma_u^+$, $^2\Sigma_g^+$, $^2\Pi_u$, and $^2\Pi_g$ states, respectively.

Figure 4 gives the evolution of the C_3^+ doublet states along the bending coordinate where both CC distances are kept fixed at 2.45 Bohr. This figure shows that C_3^+ possesses two stable isomers, cyclic c-C_3^+ and linear l-C_3^+, which are "almost isoenergetic". The PES of the electronic ground state is flat along the bending coordinate and exhibits strong vibronic couplings with the lowest $^2A_1$ component correlating with the $^2\Sigma_g^+$ state at linearity. The $^2A_1$ state is almost isoenergetic with the $^2B_2$ component. A small barrier between the bent forms and the linear isomer is found, which allows large amplitude motions to occur. To derive more accurate information for the electronic ground state, the evolution of the $^2\Sigma_u^+$ and the $^2\Sigma_g^+$ states along the bending coordinate was investigated using the MRCI method. The resulting 1-D cuts of the 3-D PESs are depicted in Figure 5. In these calculations, the R_{CC} distances were set to either 2.65 Bohr (i.e., approximately their equilibrium values in $^2A_1$; thick lines) or 2.45 Bohr (i.e., approximately their equilibrium values in $^2\Sigma_u^+$, $^2B_2$, and $^2\Sigma_g^+$; thin lines). By examining Figure 5, we confirm the bent structure of the C_3^+ in its electronic ground state (with $\theta \sim 57°$ for $^2B_2$ and $\theta \sim 65°$ for $^2A_1$), which is in good agreement with the results of Grev et al.[37] At the MRCI level of theory, the $^2\Sigma_u^+$ state is located at $\sim 770 \pm 160$ cm^{-1} (i.e., 0.09 ± 0.02 eV) above the global $^2B_2$ minimum and separated from it by a potential barrier of $\sim 100 \pm 20$ cm^{-1}. The $^2A_1$ minimum lies close in energy to the $^2B_2$ state. The energy differences of both forms are within the error bars of these computations. Our computed relative energy of the linear and the bent structures of C_3^+ are in accord with the 0.30 ± 0.17 eV value of Grev et al.[37] and 0.23 ± 0.07 eV of Taylor et al.[38] Finally, Figure 4 shows that the two Π states split, in bent geometries, into two components due to the well-known Renner−Teller effect. For instance, the $^2\Pi_u$ and the $^2\Pi_g$ states are linear/linear Renner−Teller systems. The crossings between $^2A_1$ and $^2B_2$ components are responsible for the conical intersections in the angle range of $\sim 60°-90°$. Figure 5 also provides insight into the evolution of the conical intersection between the lowest $^2B_2$ and $^2A_1$ states when both R_{CC} distances are varied symmetrically.

Discussion

Because of the energetic ablation process, the C_3 molecule can be created in various electronically excited states. The states that relax by fluorescence, such as the $\tilde{A}^1\Pi_u$ or the $^1\Sigma_u^+$ state, will not survive the few hundred microseconds flight time between the laser ablation and the ion extraction pulses. For example the $\tilde{A}^1\Pi_u$ state has a natural lifetime of 200 ± 10 ns, in the gas phase.[8,9,39] In contrast, the triplet states that undergo relaxation via phosphorescence could survive up to the ionization region. The $\tilde{a}^3\Pi_u$ and the $\tilde{b}^3\Pi_g$ states lie about 2.1 and 2.9 eV above the $\tilde{X}^1\Sigma_g^+$ state, respectively.[14,40] They can be populated in various ways during ablation, either by relaxation of higher triplet states populated by multiphoton absorption or by intersystem crossing. Becker et al.[39] assumed that a transition induced by collisions to the nearby $C_3(\tilde{b}^3\Pi_g)$ state occurs to explain the high quenching efficiency of $C_3(\tilde{A}^1\Pi_u)$ by helium. This triplet state relaxes toward the $\tilde{a}^3\Pi_u$ states via infrared emission.[14,15] Čermák et al.[13] studied the kinetics of this intersystem crossing in an Ar matrix by monitoring the rise of the $\tilde{a}^3\Pi_u-\tilde{X}^1\Sigma_u^+$ phosphorescence emission. No delay between the laser pulse and the phosphorescence emission was observed, which indicates a fast transition between the singlet and triplet manifold. The lifetime of the $\tilde{a}^3\Pi_u$ state was estimated at 50

(37) Grev, R. S.; Alberts, I. L.; Schaefer, H. F. *J. Phys. Chem.* **1990**, *94*, 3379−3381.
(38) Taylor, P. R.; Martin, J. M. L.; Francois, J. P.; Gijbels, R. *J. Phys. Chem.* **1991**, *95*, 6530−6534.
(39) Becker, K. H.; Tatarczyk, T.; Radicperic, J. *Chem. Phys. Lett.* **1979**, *60*, 502−506.
(40) Hwang, C. H.; Klassen, S. A.; MoazzenAhmadi, N.; Tokaryk, D. W. *Chem. Phys. Lett.* **1996**, *250*, 273−278.

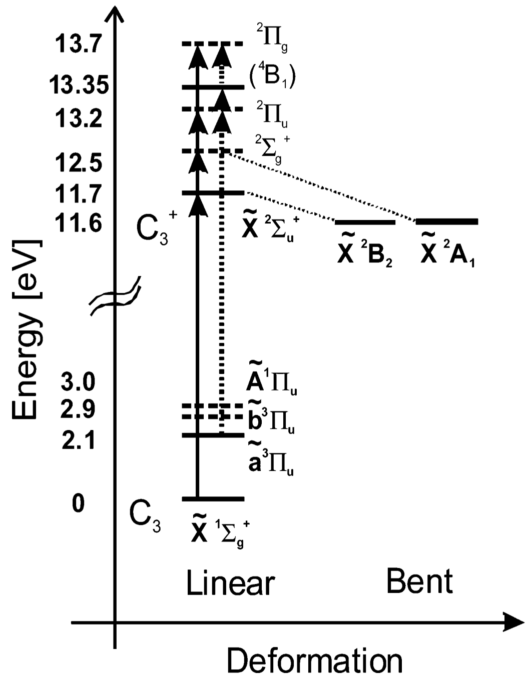

Figure 6. Energy diagram summarizing the transitions occurring when the C_3 molecular beam is ionized. Solid lines are for transitions from the $C_3(\tilde{X}^1\Sigma_g^+)$ state, and dashed lines, those from the $C_3(\tilde{a}^3\Pi_u)$ state.

μs in a gas discharge cell[14] and from 10 to 20 ms in argon and neon matrices.[13,41] The dramatic shortening of the lifetime in the gas-phase experiments[14] was attributed to collisional relaxation and reaction with C_2H_2, the precursor of C_3. If this state survives the collision regime of our supersonic expansion, its lifetime in the free collision part of our molecular beam will be bracketed between these two extreme values. Also, depending on the buffer gas used, the experimental conditions of the supersonic expansion and the timing between the opening of the pulsed valve and laser ablation will probably change the population of the $\tilde{a}^3\Pi_u$ state in the molecular beam and consequently the electronic state distribution of C_3^+ that can be reached in the single photoionization process. Figure 6 is an energy diagram summarizing the transitions that occur when C_3 is ionized by VUV light.

Given the arguments about excited states in the beam, the differences in shape of these two PIE spectra come from a change in the internal energy (most likely electronic as opposed to vibration) of the neutral C_3 beam in He and N_2. When N_2 is used as the buffer gas, the PIE exhibits a sharper rise at 12.5 eV, suggesting better cooling. The relatively low PIE signal for photon energies lower than 11.3 eV (which is distinctly below the ionization energies of C_3, see below) suggests that a miniscule percentage of C_3 ($a^3\Pi_u$) remains in our molecular beam, even when N_2 is used as the buffer gas.

The neutral C_3 molecule in its electronic ground state is a linear molecule with a very flat bending potential, and the ground $^2B_2$ state of the C_3 cation is bent.[20] This can explain the slow increase of the PIE curve at the beginning, due to unfavorable Franck−Condon factors. But when the photon energy is high enough to reach the linear geometry $C_3^+(^2\Sigma_u^+)$ electronic states, the Franck−Condon factors become very favorable, as is observed in Figure 3, and the transition probability should increase. If we assume that the first step in Figure 1a is due to the transition between the ground state of the C_3 neutral molecule and the first linear electronically excited $^2\Sigma_u^+$ state of the C_3 cation, then the value of 11.70 ± 0.05 eV would correspond to a state-to-state photoionization energy. Below we present several arguments to support this hypothesis.

The vertical IE of 11.70 ± 0.05 eV is in good agreement with the previous bracketing measurements of Rohlfing et al.[23] of 9.98−11.61 eV. It is 0.5 eV lower than the 12.1 ± 0.3 eV determined by a Knudsen cell double-focusing mass spectrometer experiment performed by Kohl and Stearns.[25] Sunil et al.[42] calculate, using self-consistent field (MC-SCF) and CI procedures, a theoretical vertical IE of 11.5 eV. The most recent calculation of an adiabatic IE (at 0 K), involving the $C_3(^1\Sigma_g^+)$ to $C_3^+(^2\Sigma_u^+)$ states, by Fura et al.[21] gives two values depending on the calculations: 12.22 eV (B3LYP/aug-cc-pVTZ) and 11.78 eV (CCSD/aug-cc-pVTZ). The coupled cluster (CCSD) value, which should be viewed as more accurate, is in very good agreement with our result.

As stressed above the most stable isomers of C_3^+ are the bent structures, and our calculations reveal the existence of a small barrier between the linear and the bent structures, so that large amplitude motions can occur at room temperature. The slow increase in the PIE curve could be attributed here to ionization leading specifically to the bent structures. Our MRCI calculations give the C_3^+ $^2B_2/^2A_1$ potential minima at 0.09 ± 0.02 eV below $C_3^+(\tilde{X}^2\Sigma_u^+)$. Assuming that the sharp onset is due to ionization to the linear $^2\Sigma_u^+$ state, an IE of 11.61 ± 0.07 eV, from $C_3(^1\Sigma_g^+)$ to $C_3^+(^2B_2/^2A_1)$, is deduced. This value is consistent with our measurement. The PIE curve starts to increase at a photon energy of 11.4 eV (Figure 1) for both buffer gases. Ramanathan et al.[22] measured an experimental adiabatic IE, 1.6 eV higher in energy, with a Fourier Transform Ion Cyclotron Resonance mass spectrometer. This adiabatic value is in agreement with early experimental (12.6 ± 0.6 eV [26]) and theoretical determinations (12.7 eV [43] and 12.94 eV[44]). The high value of Ramanathan et al.[22] could possibly be explained by incomplete thermalization of C_3^+ before the charge-transfer reaction, which could lead to an overestimation of the IE value. These high IE values are also in disagreement with the jet cooled study of Lemire et al.[45] They reported an upper experimental limit of the adiabatic IE equal to 12.0 eV due to an abrupt cutoff in their spectroscopic signal below this point.

The difference in shapes between the two PIE spectra in Figure 1 supports the presence of electronically excited states in the neutral beam with He as the buffer gas. As shown by previous matrix studies, vibrational relaxation of the $\tilde{a}^3\Pi_u$ state is very fast (no vibrational bands could be observed). Also the differences in the PIE spectra could be due to the opening of new ionization channels. For simplicity, we will consider only transitions occurring in the Franck−Condon region leading to favorable FC factors (i.e., forming mostly linear C_3^+ by ionizing C_3 ($\tilde{X}^1\Sigma_g^+$ and $\tilde{a}^3\Pi_u$)). Nevertheless, contributions of transitions to the bent structures after large amplitude motions in C_3^+, as stressed above, cannot be excluded.

(41) Weltner, W.; McLeod, D. *J. Chem. Phys.* **1964**, *40*, 1305−1316.
(42) Sunil, K. K.; Orendt, A.; Jordan, K. D.; Defrees, D. *Chem. Phys.* **1984**, *89*, 245−256.
(43) Williams, G. R. J. *Chem. Phys. Lett.* **1975**, *33*, 582−584.
(44) Romelt, J.; Peyerimhoff, S. D.; Buenker, R. J. *Chem. Phys. Lett.* **1978**, *58*, 1−7.
(45) Lemire, G. W.; Fu, Z. W.; Hamrick, Y. M.; Taylor, S.; Morse, M. D. *J. Phys. Chem.* **1989**, *93*, 2313−2319.

In Figure 1a, the vertical bars correspond to the spacing in energy between the doublet states of C_3^+, derived from our CASSCF calculations. The calculations provide better differences in energies between the electronic states compared to absolute ionization energies. With these differences fixed, an energy offset is applied to all three bars, to obtain the best fit to all the structures observed in the PIE data. The best agreement gives a position of 11.7 eV for the $C_3^+(^2\Sigma_u^+)$ state, which reinforces our state-to-state photoionization value of 11.7 ± 0.05 eV. The second plateau onset is in good agreement with the energy difference between the $^2\Sigma_u^+$ and the $^2\Sigma_g^+$ states. This, we believe, is the first experimental evidence for this electronically excited $^2\Sigma_g^+$ state. We note that the highest experimental IEs measured previously[22,26] correspond to the beginning of the second plateau, around 13.0 eV. This suggests that the neutral C_3 molecule may have been electronically excited in those earlier measurements. The gradual rise of the second step is probably due to the unfavorable photoionization selection rule (g↔g) between the $C_3(^1\Sigma_g^+)$ and $C_3^+(^2\Sigma_g^+)$ states.

Using N_2 as the buffer gas, the position of the $C_3^+(^2\Pi_u)$ state at 13.2 eV does not show any obvious structure in the PIE curve. On one hand, vibronic interactions may play a role in obscuring the precise positions of the electronic states. Moreover, the relatively different equilibrium geometries of $^2\Pi_u$ in contrast to $C_3(\tilde{X}^1\Sigma_g^+)$ may complicate the precise identification of the position of the vibrational states of $^2\Pi_u$. On the other hand, there is a clear increase in the PIE intensity above 13.2 eV when He is used as a buffer gas. As mentioned earlier, triplet states could be populated in the He carrier gas due to incomplete quenching. This might explain why there is an increase in intensity beyond 13.2 eV. However, to go from $C_3(\tilde{a}^3\Pi_u)$ to the $C_3^+(^2\Pi_u)$ state, a rearrangement of an electron between a π orbital and a σ orbital is needed in addition to the removal of an electron. This is unlikely to happen suggesting that transitions to other electronic states might be needed to explain the change in shape of the PIE curve at 13.2 eV. A quartet state like the $^4B_1$ state, located around 1.66 eV[21] above the $C_3^+(^2\Sigma_u^+)$ state, could be a good candidate.

Conclusion

Photoionization efficiency curves for the C_3 molecule, which is produced by laser ablation, have been measured from 11.0 to 13.5 eV. The use of different buffer gases allowed better cooling of the electronically excited C_3 molecules that are formed during the ablation process. The step structure in the PIE curve, obtained with N_2 as the carrier gas, supports a very effective cooling of the neutral C_3 molecule into its linear $^1\Sigma_g^+$ ground state. Using the experimental results, complemented by ab initio calculations, we suggest a state-to-state vertical ionization energy of 11.70 ± 0.05 eV between the $C_3(\tilde{X}^1\Sigma_g^+)$ and the $C_3^+(\tilde{X}^2\Sigma_u^+)$ states. New potential energy surfaces for the doublet states of the cation along the CC distance and the bending angle are calculated. Our calculations confirm the bent structure of C_3^+ in its ground electronic state. The second step in the PIE curve observed with N_2 as the buffer gas could be the first experimental evidence of the $C_3^+(^2\Sigma_g^+)$ excited state. This state correlates to a stable $^2A_1$ state lying very close to the already known $^2B_2$ ground state. Using these calculations in conjunction with our experimental results, a ionization energy of 11.61 ± 0.07 eV, between the neutral and ionic ground states of C_3, is deduced. A gradual increase at the onset of the PIE curve suggests a geometry difference between the ground neutral and cation states.

Acknowledgment. This work was supported by the Director, Office of Energy Research, Office of Basic Energy Sciences, Chemical Sciences Division of the U.S. Department of Energy under Contract No. DE-AC02-05CH11231. This research used resources of the National Energy Research Scientific Computing Center, which is supported by the Office of Science of the U.S. Department of Energy under Contract No. DE-AC03-76SF00098.

Supporting Information Available: Complete ref 36. This material is available free of charge via the Internet at http://pubs.acs.org.

JA055430+